Water Air Soil Pollut (2007) 179:283–296
DOI 10.1007/s11270-006-9231-x

RESEARCH PAPER

A Morphometric and Compositional Approach to the Study of Ambient Aerosol in a Medium Industrial Town of Italy

Giovanni Pratesi · Matteo Zoppi · Thomas Vaiani · Francesca Calastrini

Received: 1 March 2006 / Accepted: 23 June 2006 / Published online: 14 December 2006

Abstract Morphometric and compositional studies have been performed on both $PM_{10–2.5}$ and $PM_{2.5}$ aerosol collected in the city of Prato, Italy. Chemical analysis has been carried out using PIXE technique and factor analysis was applied for the source apportionment process. Industrial emissions, vehicular traffic as well as crustal dust and marine aerosol were the sources identified. SEM-EDS analysis has been employed to individually characterize particles collected during a week of the sampling campaign. The morphometric study, performed on 43,671 particles, revealed that, for both the fine and coarse fraction, about 2/3 of particles display a high roundness coefficient, 1/3 of them a medium value, while only a small number of particles (from silicates and organics) exhibits a low roundness coefficient. Similarly, particles with small surface area represent the greater portion in both fractions. Particles classified as organics, metals and oxides, chlorides, carbonates, phosphates, sulphates and silicates have been detected in the $PM_{10–2.5}$ while in the $PM_{2.5}$ chlorides and phosphates are lacking. Silicates are about the same percentage, by concentration number, in the coarse and fine fraction (20.7% and 20.5% respectively) showing that this material, at least one fifth of the total PM, might be the result of crustal erosion and anthropic activities. The purpose of this work has been that of providing a contribution to the study of particulate matter and took an effort for relating morphometric and compositional features of urban aerosol collected in a medium size industrial city.

Keywords $PM_{10–2.5}$ · $PM_{2.5}$ · morphometry
PIXE · SEM

G. Pratesi
Dipartimento di Scienze della Terra,
Università di Firenze, via La Pira 4,
50121 Florence, Italy

G. Pratesi
CESPRO, via Galcianese 20/H,
59100 Prato, Italy

M. Zoppi (✉) · T. Vaiani · F. Calastrini
Fondazione Prato Ricerche,
via Galcianese 20/H,
59100 Prato, Italy
e-mail: m.zoppi@pratoricerche.it

1 Introduction

Particulate matter in ambient air is nowadays recognized as one of the biggest problems that concern cities of the industrialized countries. The undeniable effect of its diffusion is the growing number of people affected by health problems involving respiratory and cardiocirculatory apparatus (Dockery et al., 1993; Pagano, De Zaiacomo, Scarcella, Bruni, & Calamosca, 1996; Schwartz, Dockery, & Neas, 1996). In the many studies carried out to understand the physical and chemical nature of ambient aerosol, and the processes that are responsible for their formation and diffusion,

aerosol particles are commonly modelled as spheres so as to favour straightforward calculations of their geometrical properties and physical behaviour. Particles collected on filters used for sampling urban air display, however, a very large number of shapes and sizes (Ebert, Inerle-Hof, & Weinbruch, 2002; Ebert, Weinbruch, Hoffmann, & Ortner, 2004; Shi et al., 2003; Willis, Blanchard, & Conner, 2002, and references therein). Disregarding this variety might result in not considering adequately the effects of processes like absorption of volatile molecules of pollutants and water, chemical reactivity and gravitational settling. Even though there are studies addressed to individually characterize PM (Blanco et al., 2003; Krueger, Grassian, Cowin, & Laskin, 2004; Sitzmann, Kendall, Watt, & Williams, 1999) not enough attention is commonly given to the morphometric features. The aim of this work is that of approaching the problem of the ambient aerosol in the city of Prato, Italy, from the point of view of the morphometric and compositional characteristics of its particles, and show possible relationships with atmospheric conditions.

The city of Prato is located 20 km north-west of Florence, in the proximity of the Appennines chain, and around 70 km from the shore of the Tyrrhenian Sea (Figure 1). The metropolitan area is delimited north-east and east by the Calvana mounts (about 900 m a.s.l.), a ridge made of early Caenozoic marls and limestone, and south by the Arno River plain with the high traffic highway (A11) leading from Florence to the Tyrrhenian coast. About 6 km east from the centre of the city the most heavily travelled national highway (A1) runs north–south across Italy. Prato, with about 180,000 inhabitants at the present time, is an important industrial centre of Tuscany region with active textiles, manufacturing (mostly metals and furniture), chemical and mechanical sectors. Textile industry has been the leading sector until nowadays and the town has grown constantly around factories, thus making difficult to distinguish between urban and industrial areas. No power plants are present in the area but a factory for the production of cement is located south-east, about 6 km from the centre (Figure 1). The growing traffic flow of Prato, and industry contribution to atmospheric pollution, have raised attention to the urban air quality and the replacement of oil with natural gas, for domestic and industrial use, has been almost completed. With the encouragement of the Associazione Toscana Asmatici Allergici 'Lapo Tesi' (Tuscan Association of Allergic Asthmatics) this work was started by collecting gas emissions, particulate matter samples, and performing PIXE analyses with the aim of evaluating the air quality of the town and its effects on the population. For studying the aspect of PM morphometry a part of samples has been afterwards recovered and an individual scanning electron microscopy study has been carried out.

2 Sampling and Meteorological Data

The particulate matter was collected separately at two sites (Figure 1), at a distance of about 2.5 km from

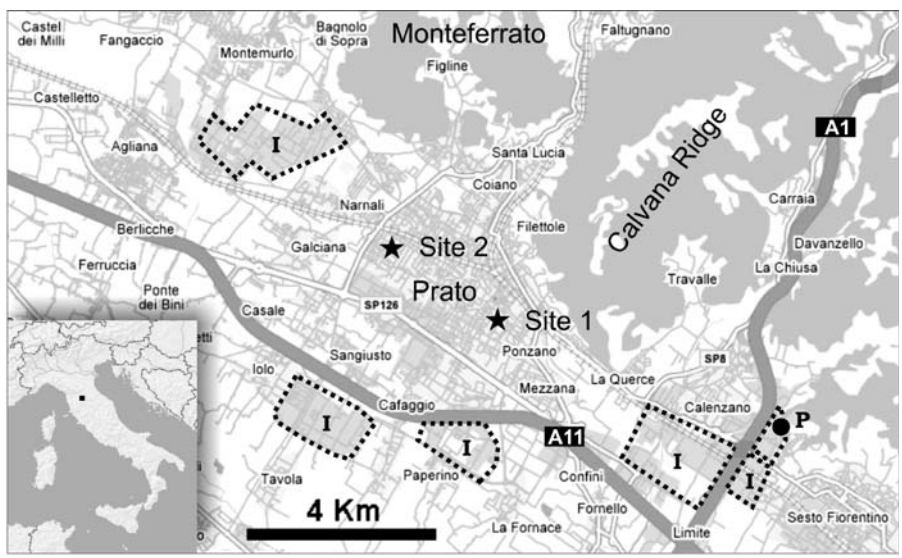

Figure 1 The metropolitan area of the city of Prato with main roads, sampling sites, suburban industrial areas (*I*), and cement production plant (*P*). The frame on the lower left corner shows the map of Italy with the location of the city.

each other, during three intervals of time, of eight days each, in the year 1999. The first sampling campaign was held between January 21st and 28th, the second between February 9th and 16th and the third between July 29th and August 5th. The 'site 1' (Ferrucci) was located along a main road in a high traffic area at the centre of the town, while the 'site 2' (S. Paolo) was located in a suburban low traffic area at the west side of the town. The two sampling stations are used for daily air quality control by the regional Environmental Protection Agency (ARPAT) and, according to the present European regulation (2001/752/EC), both are located in an 'urban' type of area; the first is classified as 'traffic' type of station, labelled 'UT', while the second as 'background' type of station, labelled 'UB'. The criteria adopted for this classification are based on the kind of dominant emission sources: determined predominantly by nearby motor vehicle traffic, for the UT stations; not influenced significantly by any single source or street, but rather by the integrated contribution from all sources upwind, for the UB stations. According to the Italian regulation on air pollution in force at the time of sampling (Italian Ministry Decree, 20 May 1991) the two stations were classified as type 'C' and 'B' respectively. Daily average concentrations, measured gravimetrically, of ambient air PM_{10} collected during the three periods are reported in Table I along with PIXE data.

A two-stage streaker sampler, provided by PIXE International Corporation[1], and the control unit have been used for urban aerosol collection as fully described in the work of Formenti, Prati, Zucchiatti, Lucarelli, and Mandò (1996). The streaker includes a pre-impactor that stops particles with aerodynamic diameter $D_{ae} > 10$ μm, a Kapton impactor that collects particles with 2.5 μm $< D_{ae} <$ 10 μm (coarse stage or $PM_{10-2.5}$) and a Nucleopore filter that stops particles with $D_{ae} < 2.5$ μm (fine stage or $PM_{2.5}$). The Kapton impaction plate and the Nuclepore filter are paired on a cartridge, which slowly rotates continuously, at an angular speed of about 45°/day. The sampling period produces a circular continuous deposit ('streak') on each of the two stages. Point by point analysis of the streak is then accomplished in order to obtain hourly information such as particle number concentration and elemental composition. The airflow of the sampler was set to a low value, 0.7 l min^{-1}, this to maintain a constant flux and avoid to affect the particle size cut-point of the impaction stages.

Meteorological hourly data have been collected at a station located in the centre of the city, half way from the two sampling sites. For the sampling periods of January, February and July/August the daily average temperatures ranged between 1.6 and 7.6, 1.7 and 5.8, 24.3 and 27.5 °C respectively. The hourly average values of wind direction are shown, along with the wind direction frequencies, in the histograms of Figure 2. The weather conditions for the period of January 21st–28th were mostly of high pressure, low wind velocity and presence of thermal inversion. The beginning of the period of February 9th–16th was coincident with the interaction of warm humid air mass, from SE, and a cold front from NE that caused a snow fall during the first and the second day. Variable values of relative humidity and temperature were recorded through the week, and atmospheric pressure was constantly increasing from the second to the seventh day. The period between July 29th and August 5th was characterized by stable weather conditions, no thermal inversion and constant atmospheric pressure (1,004–1,006 mbar).

3 Measurements and Methods

3.1 PIXE analysis

Elemental chemical analysis of the samples has been carried out with 3 MeV protons using the PIXE beam facility (Johansson & Campbell, 1988) of the INFN Van de Graaf accelerator KN3000 at the Physics Department of the University of Florence, as described in Calastrini et al. (1997). PIXE spectra were fitted using the PIXAN software (Clayton, 1986) and hourly elemental concentrations of the particulate matter were obtained as usual via a calibration curve from a set of thin standards of known areal density. It was possible to perform the analysis on the following samples: coarse and fine fraction from Site 2, between January 21st and 28th; coarse and fine fraction from Site 1, between February 9th and 16th; coarse fraction from Site 2, between February 9th and 15th; and fine fraction from Site 1, between July 29th and August 5th. Chemical variations of elements such as Na, Mg,

[1] P.O. Box 2744, Tallahassee, FL 32316, USA.

Table I PIXE 24-h averaged elemental concentration (ng m^{-3}) for the fine and coarse fraction of particulate matter collected on filters

	Day	PM_{10}	Na	Mg	Al	Si	S	Cl	K	Ca	Ti	Fe	Ni	Cu	Zn	Br	Pb
Site 2, January,	21	97.7				610	204		183	745	15	397	–	14	10	–	10
Coarse fraction	22	101.8				709	288		163	964	17	451	–	15	14	–	13
	23	118.0				666	233		184	743	12	384	–	15	11	–	11
	24	105.0				616	179		195	658	9	293	–	12	9	–	12
	25	132.3				706	281		214	873	14	356	–	14	11	–	14
	26	151.9				766	178		140	1,200	24	464	–	15	14	–	15
	27	34.7				378	223		203	225	2	83	–	4	4	–	4
	28	57.6				456	133		154	572	8	170	–	7	5	–	10
Site 2, January,	21	97.7				2,142	2,259		932	567	–	492	13	24	52	47	125
Fine fraction	22	101.8				2,300	3,834		1,398	542	–	439	18	31	90	57	194
	23	118.0				2,213	2,840		1,036	385	–	334	7	21	37	59	158
	24	105.0				2,090	3,213		1,088	333	–	292	4	18	32	51	149
	25	132.3				1,141	3,920		1,330	438	–	417	23	24	70	71	183
	26	151.9				742	3,226		1,047	520	–	529	27	26	70	76	245
	27	34.7				1,453	2,853		987	395	–	195	11	13	38	47	95
	28	57.6				1,843	1,947		663	1,442	–	362	19	16	32	45	116
Site 1, February,	9	9.4	1,626	425	105	280	298	2,312	–	486	–	375	–	25	9	–	–
Coarse fraction	10		297	204	97	169	76	247	–	271	–	207	–	10	3	–	–
	11	64.2	205	169	101	275	57	146	–	521	–	286	–	11	7	–	–
	12	126.8	696	305	124	271	147	795	–	487	–	259	–	13	8	–	–
	13	26.9	333	225	119	227	68	277	–	389	–	291	–	15	8	–	–
	14	33.2	135	102	52	154	53	31	–	271	–	289	–	16	9	–	–
	15	37.9	181	157	108	259	65	48	–	437	–	318	–	16	9	–	–
	16	51.7	182	142	108	297	63	93	–	531	–	404	–	20	11	–	–
Site 1, February,	9	9.4		135	48	529	1,715	–	914	295	–	194	–	17	43	68	57
Fine fraction	10			86	56	346	962	–	142	261	–	208	–	13	18	54	44
	11	64.2		149	117	447	1,520	–	128	676	–	288	–	14	31	50	37
	12	126.8		125	99	356	1,906	–	144	446	–	305	–	16	37	51	39
	13	26.9		116	105	379	1,868	–	189	478	–	385	–	20	41	50	51
	14	33.2		135	99	369	2,710	–	301	387	–	431	–	28	63	59	80
	15	37.9		152	122	380	4,700	–	271	378	–	365	–	21	59	54	64
	16	51.7		214	135	570	4,562	–	485	729	–	652	–	31	79	71	94
Site 2, February	9	9.4	443	105	21	87	99	836	–	125	–	44	–	–	–	–	–
Coarse fraction	10		68	24	12	57	24	128	–	81	–	56	–	–	–	–	–
	11	64.2	18	22	15	51	18	20	–	102	–	30	–	–	–	–	–
	12	126.8	125	35	14	43	33	218	–	85	–	36	–	–	–	–	–
	13	26.9	24	12	5	23	7	29	–	42	–	49	–	–	–	–	–
	14	33.2	22	16	11	63	20	23	–	117	–	86	–	–	–	–	–
	15	37.9	21	16	17	56	17	7	–	107	–	60	–	–	–	–	–
	16	51.7															
Site 1, July/Aug.	29	17.3	281	231	196	618	3,931	100	175	140	–	269	–	15	35	42	50
Fine fraction	30	18.1	314	229	162	526	3,685	83	154	216	–	380	–	16	38	49	43
	31	15.2	292	251	164	508	2,314	100	156	248	–	339	–	17	27	44	28
	1	39.7	371	319	258	617	2,315	145	256	272	–	331	–	17	27	51	40
	2	26.1	319	272	238	630	3,386	95	342	404	–	496	–	28	35	55	68
	3	31.0	334	261	200	591	4,912	76	283	308	–	556	–	27	40	57	65
	4	16.4	351	242	230	679	5,592	105	352	357	–	674	–	34	61	59	86
	5	32.5	339	276	263	634	4,822	88	304	362	–	627	–	47	52	82	80

The concentration of daily ambient air PM_{10} (μg m^{-3}), as measured by ARPAT during the three periods studied, is reported on the third column. A blank cell means that the concentration was not determined; the horizontal bar means that the concentration was always below the MDL.

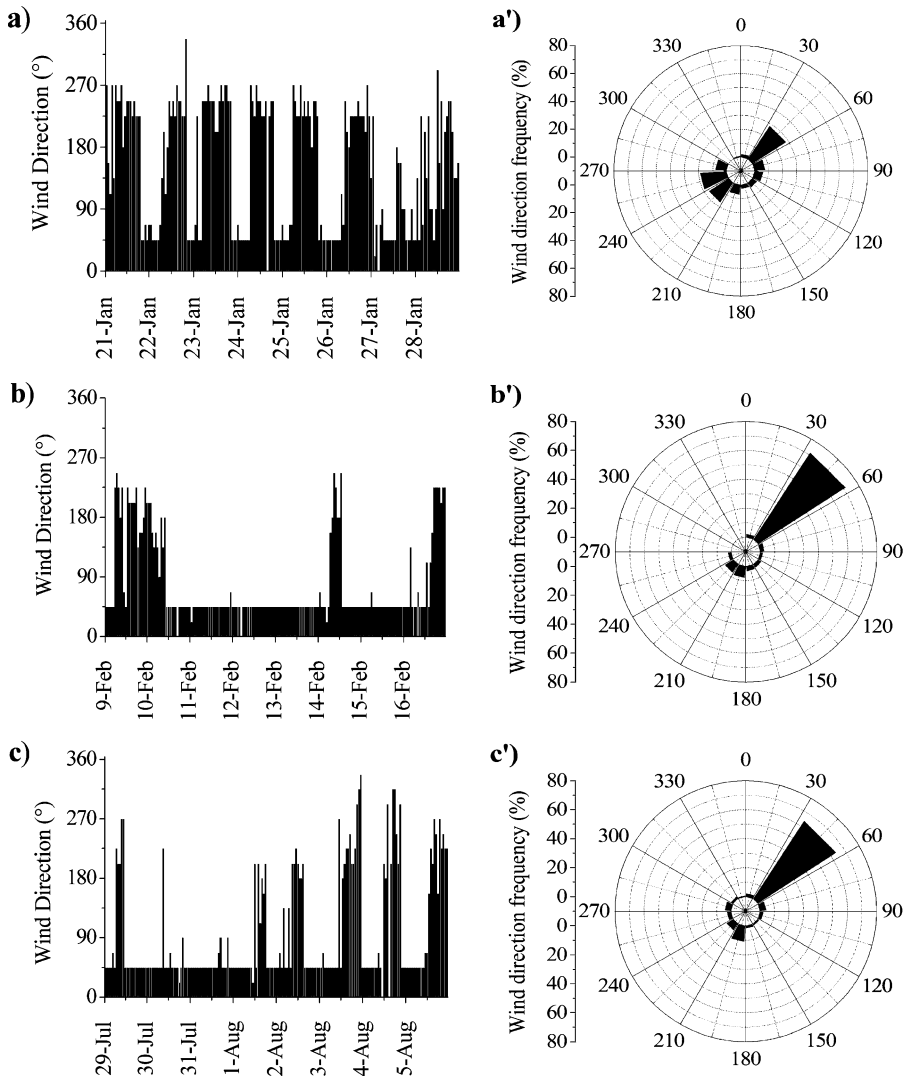

Figure 2 Wind conditions during the three sampling periods. (a), (b) and (c): Hourly averaged wind directions, in degrees; (a′), (b′) and (c′): direction frequency distribution, as percentage, for the analogous periods.

Al, Si, S, Cl, K, Ca, Ti, Fe, Ni, Cu, Zn, Br and Pb were observed. It was not possible to determine elemental concentration of Na, Mg, Al and Cl on samples of both Nucleopore and Kapton collected between January 21st and 28th at the site 2, due to technical problems. For the same reason the elemental concentration of Na of the fine fraction collected between February 9th and 16th at the Site 1 was undetermined. The lack of data for the coarse fraction at the site 2 on February 16th was due to a fracture of a small portion of the filter during the operations of preparation for analysis. Owing to the large amount of elemental concentration data, detected on hourly basis, only the calculated daily average values are reported in Table I. The uncertainties in the measurements of concentration were usually around 5%, largely due to the uncertainties on thickness of thin standard foils. Minimum detection limits (MDL) were approximately 10 ng m^{-3} for elements from Na to V and 1 ng m^{-3} (or below) for elements from Cr to Pb. To highlight correlations between the elements detected, factor analysis, with the help of the program Statgraphics Plus (1995), was applied for the source apportionment process. The results of factor analysis for all the samples analysed are summarized in Table II.

Table II Results of factor analysis form PIXE data for all the samples analysed

	F	Na	Mg	Al	Si	S	Cl	K	Ca	Ti	Fe	Ni	Cu	Zn	Br	Pb	Source
Site 2, Jan.	a1				**0.81**	0.06		0.13	**0.95**	**0.89**	**0.92**	–	**0.86**	**0.93**	–	0.47	Crustal
21st–28th,	a2				0.49	**0.91**		**0.93**	0.05	0.18	0.14	–	0.04	0.13	–	0.06	Industry
Coarse fraction	a3				0.15	0.18		0.16	0.13	0.20	0.27	–	0.39	0.24	–	**0.86**	Traffic
Site 2, Jan.	b1				0.08	0.18		0.33	0.20	–	**0.80**	0.45	**0.73**	0.35	**0.85**	**0.86**	Traffic
21st–28th,	b2				0.53	**0.87**		**0.85**	0.19	–	0.03	0.03	0.29	0.28	0.24	0.21	Industry
Fine fraction	b3				0.51	0.32		0.05	0.18	–	0.23	**0.75**	0.34	**0.80**	0.23	0.23	Industry
	b4				**0.60**	0.07		0.09	**0.86**	–	0.43	0.26	0.14	0.05	0.17	0.15	Crustal*
Site 1, Feb.	c1	**0.97**	**0.71**	0.17	0.18	**0.90**	**0.96**	–	0.15	–	0.07	–	0.28	0.08	–	–	Sea salts
9th–16th,	c2	0.14	0.01	0.04	0.29	0.19	0.16	–	0.42	–	**0.93**	–	**0.92**	0.91	–	–	Industry
Coarse fraction	c3	0.16	**0.63**	**0.91**	**0.89**	0.27	0.06	–	**0.77**	–	0.22	–	0.08	0.11	–	–	Crustal
Site 1, Feb.	d1		0.03	0.21	0.26	0.38	–	0.34	0.29	–	**0.74**	–	**0.86**	**0.75**	**0.72**	**0.89**	Traffic
9th–16th,	d2		**0.61**	**0.84**	**0.81**	0.19	–	0.03	**0.86**	–	**0.51**	–	0.29	0.21	0.04	0.23	Crustal*
Fine fraction	d3		**0.62**	0.11	0.24	**0.61**	–	**0.77**	0.07	–	0.09	–	0.13	0.32	0.37	0.18	Industry
Site 2, Feb.	e1	**0.97**	**0.88**	0.29	0.37	**0.88**	0.96	–	0.20	–	0.11	–	–	–	–	–	Sea salts
9th–16th,	e2	0.10	0.22	**0.63**	**0.83**	0.32	0.06	–	**0.82**	–	**0.79**	–	–	–	–	–	Crustal
Coarse fraction																	
Site 1, Jul.	f1	**0.85**	**0.93**	**0.88**	**0.68**	0.01	**0.81**	0.27	0.38	–	0.01	–	0.07	0.05	0.33	0.08	Crustal*, sea salts
29th–Aug. 5th,	f2	0.11	0.01	0.14	0.35	**0.83**	0.11	**0.73**	0.39	–	**0.83**	–	0.34	**0.71**	0.12	**0.65**	Industry
Fine fraction	f3	0.05	0.01	0.15	0.29	0.06	0.06	0.12	0.44	–	0.28	–	**0.88**	0.48	**0.92**	**0.61**	Traffic

For each factor *F* (in the second column), are shown in bold those elements that are considered to be significantly associated in that factor. The terms in the last column suggest the possible sources of PM. A blank cell means that elemental concentration was not determined; the horizontal bar means that the concentration was always below the MDL.

3.2 SEM-EDS analyses and morphometric data

In order to perform image analyses and collect chemical information on the single particles, scanning electron microscopy has been extensively employed using a Philips SEM 515 equipped with an energy-dispersive spectrometer (EDAX 9800). To this purpose both the Kapton impactor and the Nucleopore filter, used between February 9th and 16th, have been cut into narrow rectangular stripes, mounted on an aluminium stub with conductive carbon cement, then covered with graphitic coating. The scanning of the samples has been performed by operator control according to the following procedure. One image, with the longest side of 56 μm, has been collected for each consecutive measure of 280 μm for the whole circular length of the filter, so as to acquire a frame out of five achievable, and retain a good agreement between statistics and time employed for the analysis. Fine and coarse mode particles were identified using × 2,500 magnifications at an accelerating voltage of 20 kV. This procedure allowed the collection of 593 and 565 secondary electron (SE) images on Kapton impactor and Nucleopore filter, respectively (Vaiani, 2000). SE image analysis has been accomplished using the Video TesT-Master 4.0 program by Linear System. A total of 43,671 particles have been detected, of which 11,620 in the coarse fraction and 32,051 in the fine fraction. This software allows distinguishing each single particle from the background and calculates some parameters useful in describing its morphology. For this study, surface area A and roundness coefficient R have been chosen. The latter is defined as $4A(f^2\pi)^{-1}$, where f is the longest Feret diameter while surface area A is the measure of the particle area as it appears on the plane of the SEM image. In order to classify all the analyzed particles, according to the R parameter, three classes have been defined by choosing as extremes the following couples of values: 0 and 0.333, 0.334 and 0.666, 0.667 and 1. They have been assigned the name R_A, R_B and R_C respectively. Moreover couples of the following values of the A parameter (μm^2) have been chosen as extremes for defining six intervals: 0, 0.5, 1, 3, 6, 15 and ∞. The classes of particle surface area included between such values have been called A_A, A_B, A_C, A_D, A_E, and A_F respectively.

EDS semi-quantitative chemical analyses were performed manually on 327 particles of $PM_{2.5}$ and 309 particles of $PM_{10-2.5}$ samples. According to their

chemical composition all the particles were ascribed to one of the following eight categories: metals and oxides, chlorides, carbonates, phosphates, sulphates, silicates, agglomerates, and organics. The latter category was defined as the group of particles made of elements with atomic number $Z < 11$ and characterized by the EDS spectrum featuring a high rate of background. In this category are then included all condensible organics, ammonium nitrate as well as elemental and organic carbon. 'Agglomerates' is here considered as the group of particles that have a very variable chemical composition so that it is not possible to ascribe them to any of the mentioned categories. Their presence could be explained with the phenomenon of coalescence occurring in some cases between dust particles.

3.3 Limitations of the SEM technique

Being a non-destructive technique for qualitative elemental analysis, SEM-EDS microanalysis of particulate matter could provide valuable information (Willis et al., 2002) as long as the results are interpreted with critical attention. SEM technique, yet considering its limitations, has been considered useful in order to evaluate the geological character of PM (Moreno, Gibbons, Jones, & Richards, 2003), or determining the possible sources and its impact on monuments (Esbert, Díaz-Pache, Grossi, Alonso, & Ordaz, 2001). In the present study the first limitation, due to the instrument employed, is the lack of information about the elements with atomic number $Z < 11$. Only by removing the Be window it was possible to detect the presence of oxygen and allow the distinction between sulphates and sulphides. This operation actually led to the identification of only one particle of iron sulphide, thus considered negligible in the statistics. The other main limitation is the spatial SEM resolution, in this case approximately 0.1 μm, which effectively imposes a physical limit to the detectable fine fraction: the $PM_{2.5}$ samples have to be interpreted actually as $PM_{2.5–0.1}$. In addition the software employed for the automatic interpretation of the SE images might not identify correctly some kind of objects. Particles having dimensions in the range of 0.1–1 μm, made mostly of light elements, show a low contrast effect, making difficult to discriminate them from the background on a grey scale. The result is an underestimation, by number and composition, of light elements particles in the range of 0.1–1 μm, such as condensible organics, ammonium nitrates/sulphates, organic and elemental carbon.

4 Results

4.1 Wind circulation

The metropolitan area of Prato is often exposed to the cycle of the city–country breeze, which is favoured by the location of the city with respect to the near mounts (Figure 1), although the phenomenon might be reduced by the frequent thermal inversion occurring over the area. In case of high atmospheric pressure and stable weather conditions these phenomena control the air circulation in the area and the diffusion of pollutants. The wind behaviour of the January 21st–28th sampling period is clearly described by the bimodal character of the histograms a and a′ (Figure 2). The brightest hours of the day cause a faster warming of the vegetated slopes of the Calvana ridge and Monteferrato, with respect to the urban area, and the prevailing wind direction is about SW. As the sunlight decreases the heat accumulated by the metropolitan area is released and colder air is conveyed from NE. During the February 9th–16th sampling period, the prevailing wind direction is NE, as shown by the histograms b and b′ (Figure 2). This is caused by the unstable weather conditions already described in Section 2. Throughout the period of July 29th–August 5th the cycle of the city–country breeze was only partially occurring over the area and the prevailing wind direction was about NE (histograms c and c′ of Figure 2).

4.2 PM elemental composition and source apportionment

During the January sampling period high values of PM_{10} were detected (Table I), among the elements determined those that exhibit the highest concentrations, in both the fine and coarse fractions, are Si, S, K, Ca and Fe, but the concentrations of Si, S and K in the fine fraction by far exceed those in the coarse fraction. During the February sampling period lower values of PM_{10} are commonly detected, the elements that exhibit the highest concentrations, in both the

fine and coarse fractions, are Na, Mg, Si, Ca, and Fe, while S and K are particularly abundant in the fine fraction, and Cl is detectable only in the coarse fraction. During the same period, at the site 2, the concentrations of those elements are commonly lower. Through the period of July 29th–August 5th low values of PM_{10} are detected, the elements that exhibit the highest concentrations, in the only fine fraction, are primarily Si and S, secondarily Na, Mg, Al, K, Ca and Fe. Aerosol composition, as percent weight fraction, calculated from the data of Table I on the elemental concentration sum for each PM fraction and sampling period, is reported in the histograms of Figure 3. Generally, where the relative elemental abundances are comparable, it is to notice that Si exhibits similar values for the fine and coarse fraction, S and Ca are largely concentrated in the fine and coarse fraction, respectively. Moreover, Fe and Cu are mainly concentrated in the coarse fraction while Zn, Pb and Br are definitely concentrated in the fine fraction.

Considering the results of factor analysis, which reveals the elements significantly associated in each factor (Table II), a tentative assessment of the particulate sources was carried out. The factor a1, that associates Si, Ca, Ti, Fe, Cu and Zn in the coarse fraction, is ascribed to the crustal contribution, but the presence of Cu and Zn could be probably due to the contamination of metal dust originating from traffic (or industry). Again for the coarse fraction, also the factor c3, that associates Mg, Al, Si and Ca, as well as the factor e2, that associates Al, Si, Ca and Fe, are to be related to the crustal contribution. The factors a2 and b2 that associate S and K, as well as factor d3 that associates Mg, S and K, in both the coarse and fine fractions, are definitely a hint of anthropical activity present in the study area. Factor a3 of the coarse fraction, merely Pb, is probably to ascribe to traffic, even if the attribution is questionable. When traffic is the source this element is associated with Br, and this is commonly recognised in the factors b1, d1 and f3 that associate Fe, Cu, Zn, Br and Pb in the fine fraction. These elements are the product of motor vehicles activity (Sternbeck, Sjödin, & Andréasson, 2002; Weckwerth, 2001). Br and Pb are fuel additives still employed in Italy at the time of sampling, while Fe, Cu and Zn are due to mechanical separation of particles from the metal of the engines, and other vehicle components, undergoing friction (brake lining, tyres, etc.) and high temperatures. As known in the literature, a low Br/Pb ratio has been observed in urban areas affected by traffic, and in the nearby city of Florence, Italy, Del Carmine et al. (1999) detected values of about 0.23. The Pb detected in the coarse fraction of the January sampling period never exceeds 15 ng/m^3,

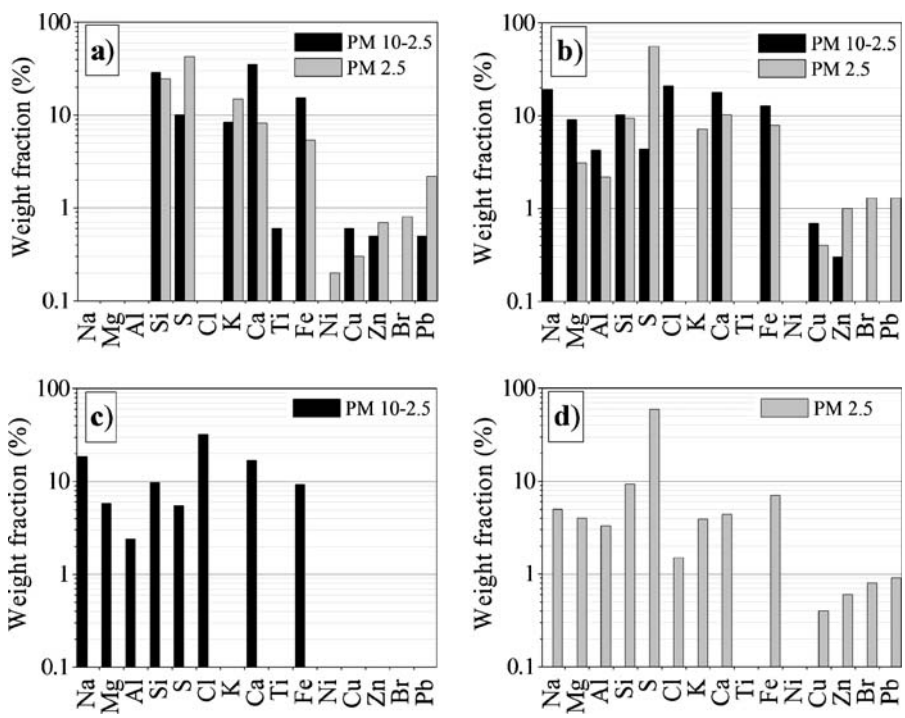

Figure 3 Aerosol elemental composition, as percent weight fraction. (a) Site 2, January 21st–28th; (b) Site 1, February 9th–16th; (c) Site 2, February 9th–16th; (d) Site 1, July 29th–August 5th.

and according to the mentioned Br/Pb ratio the corresponding amount of Br should be close to the MDL, thus hardly detectable. The factor b3, that relates Ni and Zn in the fine fraction, is considered to point out an industrial source and is probably due to the presence of some small-sized firms of metal manufacturing located in the area. The factor b4 that associates Si and Ca, and the factor d2, that associates Mg, Al, Si, Ca and Fe, are of difficult interpretation. They have been related to the crustal origin but the issue will be discussed later on. The association of Na, Mg, S and Cl, in the coarse fraction of site 1 and 2 (factor c1 and e1), during the February sampling period, was related to the presence of marine aerosol, containing chlorides and sulphates, that reaches the inland regions from the coast. Lucarelli, Mandò, Nava, Prati, and Zucchiatti (2000) and D'Alessandro et al. (2003) already observed the association of Na, Mg and Cl in the $PM_{10–2.5}$ collected in Florence and related these elements to the sea spray. The ability of this material to reach areas far from the coast has been already documented and more recently observed even for a city like Madrid, Spain (Rodríguez et al., 2004). The particularly high concentration of Na and Cl, on February 9th (Table I), is probably also due to the use of de-icing products employed because of the mentioned snow fall. The association of Fe, Cu and Zn in the coarse fraction (factor c2) is to ascribe again to the metal manufacturing industry. The July/August sampling period was characterized by a reduced traffic flow and working activity, because of summer holidays, although industrial activity was still going on. The concentrations of ambient air PM_{10} was low, the absence of thermal inversion favoured the city–country breeze effects and the dispersion of pollutants. Factor f1 shows again the relationship between Na and Cl along with Mg, Al and Si in the fine fraction. This has been interpreted as marine aerosol contaminated by crustal matter from the soil, then resuspended. Remarkable, during this period, is the concentration of S (Table I) associated with K, Fe, Zn and Pb in the factor f2, which is ascribed to industrial emissions.

4.3 Composition of the particles and morphometric studies

Particle number concentration of the fine and coarse fractions obtained from morphometric analysis are compared in the scatter chart a of Figure 4. Each point represents a pair of $PM_{2.5}$–PM_{10} average particle number concentrations detected on hourly basis. The dashed diagonal line is the 1:1 line and shows that the $PM_{2.5}$ number concentration ranges between 47% and 96% of PM_{10}. It is shown the line (continuous) of best fit regression and the detailed correlation statistics is reported in the upper-left corner of the graph. The ratio of overall $PM_{2.5}$ and PM_{10} average number concentrations is also indicated: $PM_{2.5}$ accounts for 75% of the total PM_{10}. These, and the following results, were obtained employing the SEM technique and its limitations strongly influence every kind of comparison with results obtained with other counting techniques. Studies carried out in urban and industrial areas (Stanier, Khlystov, & Pandis, 2004; Van Dingenen et al., 2004) show that number concentrations, for $PM_{2.5}$, is on average of the orders of 10^3–10^4 particles cm^{-3}, the highest values occurring chiefly for particles in the 0.1–1 μm range. These values are by far higher than those obtained in this study, affected by the kind of underestimation above mentioned (Section 3.3). The histograms b and c (Figure 4) show, respectively, the number concentration for the classes of the roundness coefficient (R parameter) and for the classes of the surface area (A parameter) of the coarse fraction ($PM_{10–2.5}$) and the fine fraction ($PM_{2.5}$) of particulate matter. Further classes of number concentration have been created by sharing the elements belonging to each surface area class (A_A to A_F) among each of the three classes of roundness coefficient (R_A to R_C) as defined above. The eighteen classes of number concentration so obtained were labelled progressively 1, 2, 3, etc., and are shown in the histogram d (Figure 4). From the histograms b and c it is clear that the number concentrations for the fine fraction are much higher than those for coarse fraction. The histogram c shows that for both coarse and fine fraction the number concentration grows exponentially for classes of lower surface area. Furthermore a very small number of $PM_{2.5}$ particles show a sharpened or acicular shape, about one third of them shows that $0.334 \leq R \leq 0.666$ and about 2/3 of the total are rounded or spherically shaped. This observation is valid for $PM_{10–2.5}$ particles as well, but the number concentration of each class is less than half of the amount of the homologous class of $PM_{2.5}$. From the histogram c it is also evident that the greatest number of particles possesses a very small surface area, actually for more

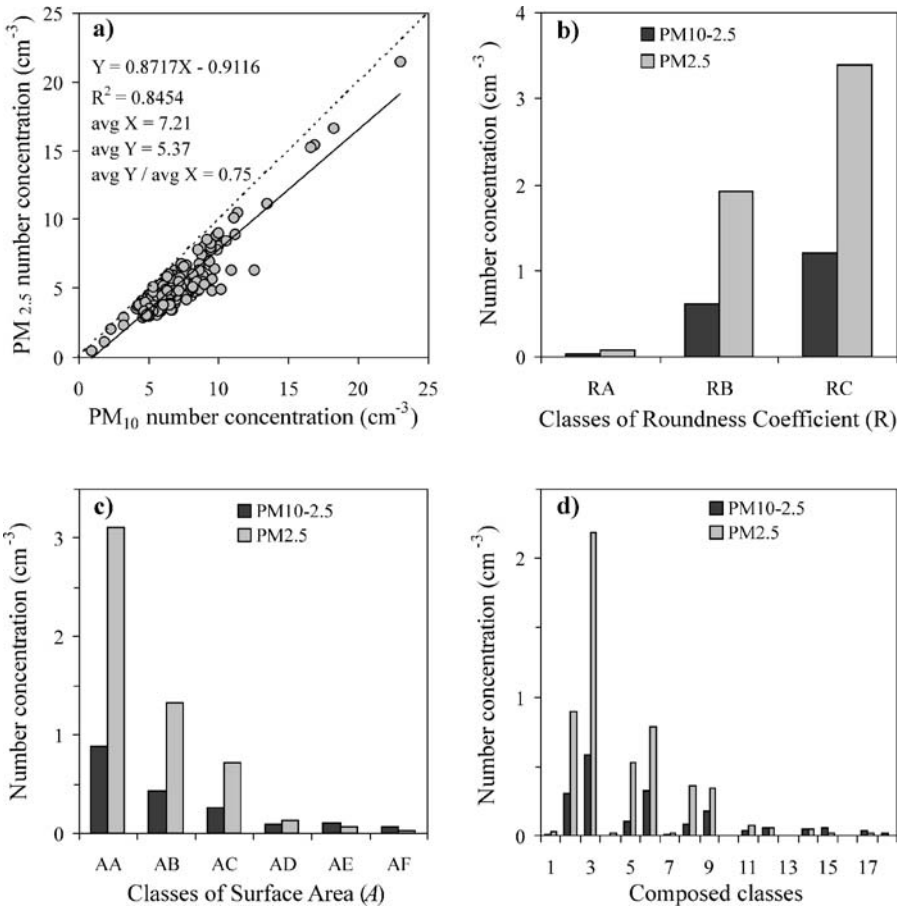

Figure 4 Statistics on the coarse and fine PM collected during the week between February 9th and 16th at Site 1. (a) $PM_{2.5}$–PM_{10} hourly average number concentration (for details see text); (b) average number concentration for the particle roundness coefficient classes R_A, R_B and R_C; (c) average number concentration for the particle surface area classes A_A, A_B, A_C, A_D, A_E, and A_F; (d) average number concentration for the particle classes obtained combining the parameters R and A (as explained in the text).

than 95% of the $PM_{2.5}$ particles $A \leq 3$ μm^2; similarly, for more than 83% of the $PM_{10-2.5}$ particles $A \leq 3$ μm^2. The number concentration for the classes A_A, A_B, A_C and A_D of $PM_{2.5}$ is higher than that for the same classes of $PM_{10-2.5}$, but for the classes A_E and A_F the number concentrations of the fine fraction is lower than that of the coarse fraction. The reason is simply that particles belonging to these two classes, that is, having a surface area higher than 6 μm^2, are likely to have $D_{ae} > 2.5$ μm, thus belonging for the most part to the coarse fraction. Particles of the fine fraction belonging to A_E and A_F classes are likely to have a density lower than unity. The histogram d (Figure 4) shows the trends already observed for the histograms b and c of both fractions.

The particle number concentration, as percentage, for each category of composition identified by SEM-EDS analysis, and detected in the coarse and fine fraction, are reported in the histograms a and b of Figure 5, respectively. Considering first the fine fraction, one might see that the majority of the particles has organic nature, about one fifth of the total are silicates, metals and oxides are 8.6% and the remaining are sulphates (largely calcium sulphate), agglomerates, and a very small amount of carbonates. The coarse fraction show the presence of chlorides and phosphates for a total of about 15%, organic particles halved their presence, with respect to the fine fraction, while carbonates, and the group of metals and oxides, have significantly higher percentages. Silicates and sulphates (largely calcium sulphate) show about the same percentages as that of the fine fraction. From these data we can see that compounds such as carbonates, chlorides and phosphates belong almost completely to the coarse fraction, while silicates and sulphates belong almost equally to both the fractions. Further attention has been given to the chemical composition of silicates, metals and oxides, and agglomerates. The silicate particles exhibit a heterogeneous chemical composition; Si and Al are

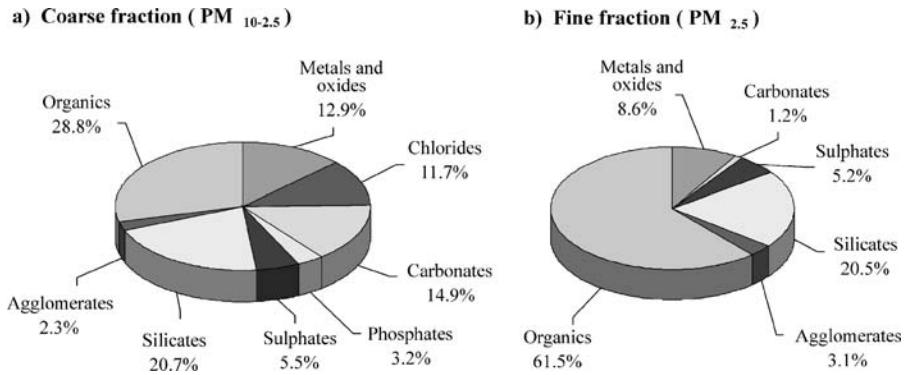

Figure 5 Particle number concentrations, as percentage, for each category of chemical composition identified by SEM analysis. (a) Coarse fraction ($PM_{10-2.5}$); (b) fine fraction ($PM_{2.5}$).

usually the most abundant elements while Na, Mg, K, Ca and Fe are detected in variable quantity. Aside from quartz and kaolinite, which have been identified by their particular chemical composition and typical morphometry, operating only with SEM the mineralogical nature of the silicate particles would result ambiguously determined. For this reason the criterion adopted was that of making a distinction between silicates and aluminosilicates, and additionally grouping the particles according to their most abundant element among Na, Mg, K, Ca and Fe. The number concentration, as percentage, for the fine and coarse fraction of PM are reported in the histogram a of Figure 6. The particles belonging to the class of 'metals and oxides', which must be intended as including hydroxides, exhibit a simple composition. Three groups are present in the coarse fraction with the following elements: Al and O; Fe and O; Fe, Cu and O (as percentage about 3%, 77%, and 20% respectively). The fine fraction is similarly composed of three groups with the elements: Pb, Br and O; Fe and O; Fe, Cu and O (about 4%, 78%, and 18% respectively). Particles classified as 'agglomerates' are few, they are composed of many elements among O, Na, Mg, Al, Si, P, S, Cl, K, Ca, Ti, V, Fe, Cu, Zn, Pb. For these Ca and Na are the most abundant in the coarse fraction while Si, Al and Ca are the most abundant in the fine fraction. A particular feature that many particles reveal, under SEM-EDS analysis, is the presence of a small quantity of S apparently spread on their surface. Aside from sulphates, S was detected only on agglomerates, rarely on the organics of the $PM_{2.5}$, but largely on

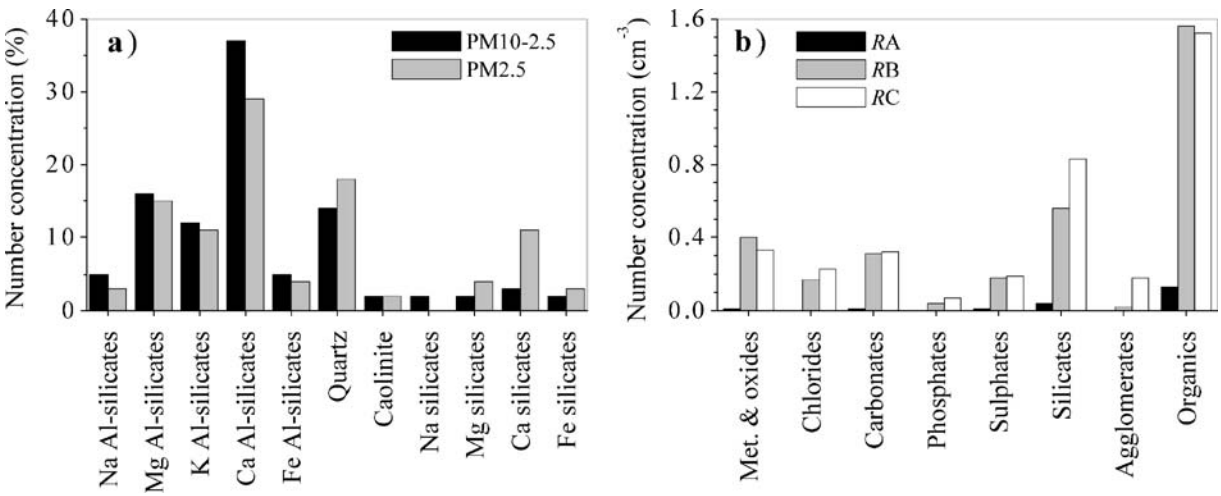

Figure 6 Results of the SEM-EDS analysis. (a) Chemical speciation of the silicate particles, in the fine and coarse fraction of PM collected during the week between February 9th and 16th at Site 1. The reported values are the number concentrations, as percentages, of each group of silicates according to the most abundant element among Al, Na, Mg, K, Ca, and Fe. (b) Number concentration for the R_A, R_B and R_C classes for each of the eight categories of chemical composition, considered on the total of the coarse and fine fraction.

silicates: on about the 47% of the silicates of the $PM_{2.5}$ and on the 20% of the $PM_{10–2.5}$ ones.

Number concentrations for the R_A, R_B and R_C classes for each of the eight compositional classes, observed on the total of PM particles, are summarized in the histogram b of Figure 6. Aside from the fact that only one particle of each group of metals and oxide, carbonates, and sulphates was detected in the R_A class, only silicates and organics show a small amount of particles with low roundness coefficients. Carbonates, phosphates, sulphates and organics display the same amount of particles for the R_B and R_C classes, while for chlorides and silicates rounded particles are the majority. Almost all particles of the agglomerates belong to the R_C class.

Further possible relationships between particulate matter and atmospheric conditions have been considered but no significant correlation or trend was observed with respect to the hourly average wind speed and direction, air temperature, pressure or relative humidity.

5 Discussion

Factor analysis and the source apportionment process for the three periods under study, point out that in the city of Prato the sources of particulate matter are mainly to ascribe to the anthropic activities, such as industrial emissions and vehicular traffic, although some significant natural contributions from crustal dust and marine aerosol are present. Materials originating from industrial activity and crustal erosion are found in both the fine and coarse fractions of PM, metals originating from vehicular traffic are detectable in the only fine fraction while those of industrial origin belong to both the fractions. Generally the particles analysed with the SEM-EDS technique exhibit a small surface area and a medium and high roundness coefficient. It is evident from the histograms a and b of Figure 5 that the organic PM represents the great majority of $PM_{2.5}$ and a remarkable part of $PM_{10–2.5}$, while the silicates are in the same amount on both fractions. A relevant part of $PM_{10–2.5}$ is due to carbonates, originated from the local geologic environment, along with chlorides, sulphates and phosphates. Commonly the mineral dust, marked by the association of Mg, Al, Si, Ca, Ti and Fe, is mainly detected in the coarse fraction of ambient aerosol. The high and equal percentage of silicates in both the fractions of our samples might suggest a possible anthropic origin of the fine silicates. The work of Moreno et al. (2003) shows that, even for two geologically different environments, the percentages of silicates of the coarse fractions are much higher that those of the fine fractions, respectively, while for sulphates the trend is opposite. The different results of the present work might be due to several reasons. The geologic environment of the study area is chiefly of carbonatic nature, while Moreno et al. (2003) examined two environments mostly of silicatic nature. The compositional data are reported as percentages, not as mass concentration, and these are influenced by the concentration of ambient air PM, which in the February sampling period displayed very variable values. The spatial resolution of the SEM employed causes an underestimation of the smallest particles and affects the percentages of the chemical compositions. In fact the EDS semi-quantitative chemical analysis was performed manually, mostly on those particles featuring high surface areas; for about 77% of them the A parameter was greater than 3 μm^2. The reason of this choice lays on the fact that for larger particles chemical analysis is more accurate and less affected by the influence of the Kapton or Nucleopore filter. Nevertheless the relative concentrations of the Si (histograms of Figure 3) confirm that this element is present in roughly the same amount in the fine and coarse fraction. Looking at the histogram a of Figure 6 it appears that among the silicates in both the fractions the more abundant are aluminosilicates and quartz. Regarding the relative concentrations of the different types only quartz, Mg, Ca and Fe silicates are more abundant in the fine fraction while aluminosilicates are slightly more abundant in the coarse one. Minerals commonly forming soil dust are quartz, clay minerals such as kaolinite (T-O silicate of aluminum), vermiculites (TOT layer aluminosilicates of A1, Fe, Mg with hydrated cations in the interlayer space), and chlorites (TOT +O layer aluminosilicates of Mg, Fe, Al), K-feldspars (aluminosilicates of K) and plagioclases (aluminosilicates of Ca and Na). In both the fractions of our samples these groups show little differences in the relative concentrations, except for the Ca-aluminosilicates. It is to say that, commonly, clay minerals particles are typically below 2–3 μm, thus belonging to the fine fraction, but also fly ashes have silicatic composition and reside in the fine fraction (Ebert et al., 2004; Shi et al., 2003). It is difficult to trace the source

of the fine silicatic PM and it cannot be ruled out that the material is a mix of natural and anthropogenic silicates (labelled with * in Table II). The cement production plant, located few kilometres east from the suburbs of the city (Figure 1), might contribute, under certain weather conditions, to the presence of silicate particles over the metropolitan area. A further consideration on the correlation of S with K might add some information. Their association might be related to the use of sulphuric acid, widely employed in the process of carbonization of wool and cotton. K is one of the main elements contained in the straw (Christensen, Stenholm, & Livbjerg, 1998), the latter being the prime impurity of the raw wool. Sulphur is actually present on the organics of the $PM_{2.5}$ aerosol, but K belongs only to the silicates, agglomerates and is rarely found on the surface of some organic particles. Since it is evident the presence of secondary sulphates on the fine silicate particles, from SEM analyses, and being secondary sulphates of anthropic origin, this might suggest the same origin as well for the silicates of the $PM_{2.5}$.

Another characteristic noticed for the class of silicates, but also for the organics, is the heterogeneous type of morphologies. Only these classes show a certain number of particles with a low roundness coefficient while this feature is practically absent in the remaining groups. The morphology of natural silicates is due to their crystal chemical nature, and during the alteration processes the crystals fracture along definite planes which give sharp and distinctive shapes. Quartz exhibits conchoidal fracture while clay minerals are found as platelet like crystals. The acicular forms are typical of inosilicates, amphiboles and minerals of asbestos, all materials which raise health concerns. The morphology of organic PM that exhibits a low roundness coefficient is instead due to a different mechanism; soot is made indeed of fractal like aggregates of spherical particles developing in chains (Ebert et al., 2004; Shi et al., 2003; Willis et al., 2002). Medium and high values of roundness coefficient are characteristics common to all groups of particles of our samples, with the exception of agglomerates that are mostly well rounded.

6 Conclusions

As it is common for many cities worldwide, the cycle of the city–country breeze and the phenomenon of thermal inversion greatly affect the dispersion of pollutants from various sources in the metropolitan area of Prato. The accumulation and recycling of pollutants in the air is probably the main event to mention for explaining higher concentrations of PM, as in the January sampling period of our study case. Some interesting elements that emerge from the study of this area are the generally high concentration of Si in the $PM_{2.5}$ ambient air, and the high amount of S, which is also related to K. The PIXE technique, still remaining of high importance, when combined with SEM technique and image analysis, could yield a more complete overview of the nature of ambient aerosol. In the city examined, a high amount of silicate particles in the $PM_{2.5}$ with the prevailing occurrence of aluminosilicates might indicate an anthropic source, but the characteristic of the metropolitan area, and the wind conditions at the sampling period, force to consider wider air circulation phenomena and possible mechanisms of accumulation of PM in the area. The correlation of S with K, and the SEM analyses that reveal the coalescence of secondary sulphates on the surface of the fine silicate particles, might suggest the anthropic origin of these materials. Moreover the image analysis and the morphometric studies allow to give useful details on the groups of particles of different composition, and focus the attention on those that exhibit particular features. The integration of PIXE and SEM-EDS techniques, with the image analysis and morphometric studies proves to be a very effective combination of tools to study the ambient aerosol.

Acknowledgments The authors wish to thank the director of the Dipartimento Provinciale A.R.P.A.T. of Prato, Dr. Luciano Giovannelli. Acknowledgments are due to: Prof. Pier Andrea Mandò and Prof. Franco Lucarelli (Dipartimento di Fisica, Università di Firenze), Dr. Mario Paolieri (M.E.M.A., Università di Firenze), Dr. Luca Matassoni (Prato Ricerche), and to the Associazione Toscana Asmatici Allerigici 'Lapo Tesi'. This work has been undertaken with the financial contribution of the Provincia di Prato.

References

Blanco, A., De Tomasi, F., Filippo, E., Manno, D., Perrone, M. R., Serra, A., et al. (2003). Characterization of African dust over southern Italy. *Atmospheric Chemistry and Physics, 3*, 2147–2159.

Calastrini, F., Barbaro, A., Del Carmine, P., Grechi, D., Lucarelli, F., Mandò, P. A., et al. (1997). Pollution sources in an

industrial urban area detected by means of air particulate sampling and subsequent analysis with PIXE and PIGE techniques. In A. Brebbia, H. Power, & T. Tirabassi (Eds.), *Air pollution V, transactions on ecology and the environment 21*. UK: Wessex Institute of Technology.

Christensen, K. A., Stenholm, M., & Livbjerg, H. (1998). The formation of submicron aerosol particles, HCl and SO_2 in straw-fired boilers. *Journal of Aerosol Science, 29*, 421–444.

Clayton, E. (1986). PIXAN: The Lucas Heights Pixe Analysis Computer Packages. Australian Atomic Energy Commission, AAEC/M113.

D'Alessandro, A., Lucarelli, F., Mandò, P. A., Marcazzan, G., Nava, S., Prati, P., et al. (2003). Hourly elemental composition and sources identification of fine and coarse PM_{10} particulate matter in four Italian towns. *Journal of Aerosol Science, 34*, 243–259.

Del Carmine, P., Lucarelli, F., Mandò, P. A., Valerio, M., Prati, P., & Zucchiatti, A. (1999). Elemental composition of size-fractionated urban aerosol collected in Florence, Italy: Preliminary results. *Nuclear Instruments and Methods in Physics Research, B150*, 450–456.

Dockery, D. W., Pope, C. A. III, Xu, X., Spengler, J. D., Ware, J. H., Fay, M. E., et al. (1993). An association between air pollution and mortality in six US cities. *New England Journal of Medicine, 329*, 1753–1759.

Ebert, M., Inerle-Hof, M., & Weinbruch, S. (2002). Environmental scanning electron microscopy as a new technique to determine the hygroscopic behaviour of individual aerosol particles. *Atmospheric Environment, 36*, 5909–5916.

Ebert, M., Weinbruch, S., Hoffmann, P., & Ortner, H. M. (2004). The chemical composition and complex refractive index of rural and urban influenced aerosols determined by individual particle analysis. *Atmospheric Environment, 38*, 6531–6545.

Esbert, R. M., Díaz-Pache, F., Grossi, C. M., Alonso, F. J., & Ordaz, J. (2001). Airborne particulate matter around the Cathedral of Burgos (Castilla y León, Spain). *Atmospheric Environment, 35*, 441–452.

Formenti, P., Prati, P., Zucchiatti, A., Lucarelli, F., & Mandò, P. A. (1996). Aerosol study in the town of Genova with a PIXE analysis. *Nuclear Instruments and Methods in Physics Research, B113*, 359–362.

Johansson, S. A. E., & Campbell, J. L. (1988). *PIXE: A novel technique for elemental analysis*. Chichester: Wiley.

Krueger, B. J., Grassian, V. H., Cowin, J. P., & Laskin, A. (2004). Heterogeneous chemistry of individual mineral dust particles from different dust source regions: The importance of particle mineralogy. *Atmospheric Environment, 38*, 6253–6261.

Lucarelli, F., Mandò, P. A., Nava, S., Prati, P., & Zucchiatti, A. (2000). Elemental composition of urban aerosol collected in Florence, Italy. *Nuclear Instruments and Methods in Physics Research, B161–163*, 819–824.

Moreno, T., Gibbons, W., Jones, T., & Richards, R. (2003). The geology of ambient aerosols: Characterising urban and rural/coastal silicate $PM_{10-2.5}$ and $PM_{2.5}$ using high-volume cascade collection and scanning electron microscopy. *Atmospheric Environment, 37*, 4265–4276.

Pagano, P., De Zaiacomo, T., Scarcella, E., Bruni, S., & Calamosca, M. (1996). Mutagenic activity of total and particle-sized fractions of urban particulate matter. *Environmental Science and Technology, 30*, 3512–3516.

Rodríguez, S., Querol, X., Alastuey, A., Viana, M., Alarcon, M., Mantilla, E., et al. (2004). Comparative PM_{10}–$PM_{2.5}$ source contribution study at rural, urban and industrial sites during PM episodes in Eastern Spain. *Science of the Total Environment, 328*, 95–113.

Schwartz, J., Dockery, D. W., & Neas, L. M. (1996). Is daily mortality associated specifically with fine particles? *Journal of the Air and Waste Management Association, 46*, 927–939.

Shi, Z., Shao, L., Jones, T. P., Whittaker, A. G., Lu, S., Bérubé, K. A., et al. (2003). Characterization of airborne individual particles collected in an urban area, a satellite city and a clean air area in Beijing, 2001. *Atmospheric Environment, 37*, 4097–4108.

Sitzmann, B., Kendall, M., Watt, J., & Williams, I. (1999). Characterisation of airborne particles in London by computer-controlled scanning electron microscopy. *Science of the Total Environment, 241*, 63–73.

Stanier, C. O., Khlystov, A. Y., & Pandis, S. N. (2004). Ambient aerosol size distributions and number concentrations measured during the Pittsburgh Air Quality Study (PAQS). *Atmospheric Environment, 38*, 3275–3284.

Statgraphics Plus© Copyright 1995. Manugistic Inc., 2115 Jefferson Street, Rockville, MD 20852, USA.

Sternbeck, J., Sjödin, A., & Andréasson, K. (2002). Metal emissions from road traffic and the influence of resuspension – results from two tunnel studies. *Atmospheric Environment, 36*, 4735–4744.

Vaiani, T. (2000). Morfometria e composizione chimico-mineralogica del particolato aerodisperso inalabile campionato nella città di Prato in una stazione di monitoraggio di qualità dell'aria di tipo "C" e relazioni con le condizioni meteoclimatiche. Tesi di Laurea, Università di Firenze.

Van Dingenen, R., Raes, F., Putaud, J.-P., Baltensperger, U., Charron, A., Facchini, M.-C., et al. (2004). A European aerosol phenomenology-1: Physical characteristics of particulate matter at kerbside, urban, rural and background sites in Europe. *Atmospheric Environment, 38*, 2561–2577.

Weckwerth, G. (2001). Verification of traffic emitted aerosol components in the ambient air of Cologne (Germany). *Atmospheric Environment, 35*, 5525–5536.

Willis, R. D., Blanchard, F. T., & Conner, T. L. (2002). Guidelines for the application of SEM/EDX analytical techniques to particulate matter samples. EPA-600/R-02-070. Research Triangle Park, NC 27711.